

Article

LEO-Assisted Aerial Deployment in Post-Disaster Scenarios Using a Combinatorial Bandit and Genetic Algorithmic Approach

Ehab Mahmoud Mohamed ^{1,*}, Sherief Hashima ^{2,3}, Kohei Hatano ^{2,4} and Haithem S. Khallaf ⁵

- ¹ Department of Electrical Engineering, College of Engineering in Wadi Addawasir, Prince Sattam Bin Abdulaziz University, Wadi Addawasir 11991, Saudi Arabia
- ² Computational Learning Theory Team, RIKEN-Advanced Intelligence Project (AIP), Fukuoka 819-0395, Japan; sherief.hashima@riken.jp (S.H.); hatano@inf.kyushu-u.ac.jp (K.H.)
- ³ Engineering Department, NRC, Egyptian Atomic Energy Authority, Cairo 13759, Egypt
- ⁴ Department of Informatics, Kyushu University, Fukuoka 819-0395, Japan
- ⁵ Reactors Department, Nuclear Research Center, Egyptian Atomic Energy Authority (EAEA), Inshas 13759, Egypt; khallafh@mcmaster.ca
- * Correspondence: ehab_mahmoud@aswu.edu.eg
- † These authors contributed equally to this work.

Abstract: This paper proposes integrating low earth orbit satellites (LEO-Sats) and multiple aerals to provide rescue services in post-disaster areas. Aerials are distributed to provide wireless connectivity to survivors and rescue workers, while LEO-Sat exhibits backhaul linkages to aerials to connect them with the closest surviving ground base station (GBS). In this context, the aerials' deployment should maximize the total system rate while guaranteeing fairness among the served post-disaster regions within aerials' limited battery budget and LEO-Sat's limited bandwidth resources. Therefore, a combinatorial bandit model with arms fairness and budget constraints (CB-FBC) is proposed to address the aerials' deployment while maintaining fairness in covering post-disaster regions within the aerials' limited battery resources. Additionally, the aerials' transmit communication powers and LEO-Sat's bandwidth resources are optimized according to traffic requests of LEO-aerial linkages using a genetic algorithm (GA). By means of numerical analysis, the proposed GA shows superior performance over other naïve benchmarks.

Keywords: genetic algorithm; LEO satellite; multi-armed bandit; combinatorial bandits; aerials



Citation: Mohamed, E.M.; Hashima, S.; Hatano, K.; Khallaf, H.S.

LEO-Assisted Aerial Deployment in Post-Disaster Scenarios Using a Combinatorial Bandit and Genetic Algorithmic Approach. *Electronics* **2023**, *12*, 4964. <https://doi.org/10.3390/electronics12244964>

Academic Editor: Jose Eugenio Naranjo

Received: 16 October 2023
Revised: 28 November 2023
Accepted: 7 December 2023
Published: 11 December 2023



Copyright: © 2023 by the authors. Licensee MDPI, Basel, Switzerland. This article is an open access article distributed under the terms and conditions of the Creative Commons Attribution (CC BY) license (<https://creativecommons.org/licenses/by/4.0/>).

1. Introduction

Due to their flying, maneuvering, and hovering merits, aerials have been increasingly used as wireless communication platforms, especially for post-disaster aid services. This is due to their ability to quickly reach remote and hard-to-access areas [1–3]. In post-disaster situations, aerials can offer wireless connection for user devices (UDs) owned by survivors and rescue teams where the terrestrial wireless communication networks are completely damaged or malfunctioned [4–7]. Deploying multiple aerials in such scenarios is challenging, requiring multi-objective optimization, including coverage, limited aerial battery life times, heights, and communication performance. Also, the limited transmission coverage of aerials might hinder their ability to establish communication links with the closest ground base station (GBS) or even among themselves, affecting their arrangement and data collection abilities in post-disaster zones.

Therefore, this paper proposes the usage of low earth orbit satellite (LEO-Sat) to assist aerials in rescue missions by creating backhaul links with the nearest survival GBS. Recently, LEO-Sat has garnered significant interest and is currently the subject of ongoing research in diverse wireless communication applications [8–15]. However, limited research studies have explored the potential integration of LEO-Sat and aerial technologies to leverage

both benefits and establish more efficient wireless communication platforms [16–18]. In the proposed post-disaster scenario, LEO-Sat effectively assists disseminating/collecting control information and data traffic to/from nearby GBSs via aerials, where only indirect communication links between GBSs and aerials exist. The primary difficulty in this system is how to effectively distribute aerials in the sparsely populated sub-areas, i.e., disaster area clusters/grids. In this scenario, the main objective is to maximize the area's total achievable sum data rates plus maintaining fairness in post-disaster cluster coverage. Also, the bounded aerials' battery capacity and LEO-Sat bandwidth should be anticipated. To ensure fairness in post-disaster cluster coverage, higher user density clusters/grids should be served more frequently than the less-populated ones. This optimization problem has three main challenges. Firstly, coverage fairness should be maintained among post-disaster clusters according to their users' densities, where the wireless infrastructure is entirely malfunctioning, which involves the difficulty of knowing victims' information. Secondly, aerials should conserve their battery energy while maximizing the collected data from the post-disaster zone to prolong their critical rescue operation cycle before recharging. Finally, optimizing aerials' transmit (TX) communication powers as well as LEO-Sat bandwidth resources according to the aerials' traffic reflects another critical challenge. To deal with this highly challenging problem, this work presents the following main contributions:

- We propose to split the LEO-Sat assisted aerials deployment problem into two sub-problems. This is enabled by aerials' TX powers towards the LEO-Sat, and the LEO-Sat bandwidth resources should be allocated based on aerials' traffic needs after deployment. In this regard, the first sub-problem deals with the limited battery budget fair aerials deployment, and the second one deals with optimizing the aerials' TX powers and LEO-Sat bandwidth resources according to the aerials' traffic needs.
- A budget-constrained combinatorial multi-armed bandit (MAB) game with arms' fairness (CB-FBC) [19] will be proposed to address the first sub-problem. In this context, MAB is an advanced online learning tool where a player intends to increase his achievable profit via playing over the bandit's arms. Only through the exploitation–exploration process, without knowing any prior knowledge about the game, the player learns how to always play with the highest-profited arm. In the sub-problem considered, the MAB player will be the nearest survival GBS, the arms will be the post-disaster clusters, and the rewards are the aerials' achievable data rates.
- To ensure fairness in clusters coverage based on users' densities, we propose that GPS localization will be used to pre-estimate users' locations, which will be refined through the aerials' exploration during the proposed combinatorial MAB game.
- In the second sub-problem and after distributing the aerials among clusters, a genetic algorithm (GA) approach [20] will be utilized to optimize the aerials' TX powers and LEO-Sat's bandwidth resources based on the aerials' traffic coming from users' loads in their covered clusters. GA is a well-known optimization algorithm that can effectively address constrained non-linear optimization problems by means of penalty hypothesis.
- Extensive numerical analysis is conducted to confirm the effectiveness of the envisioned approach against benchmark schemes, including basic MAB approaches.

The remainder of this paper is arranged as follows: Section 2 summarizes LEO-Sat aerial-related works. Section 3 previews the envisioned system model of LEO–aerial integration followed by optimization problem formulation. Section 4 figures out the proposed “CB-FBC” algorithm and “GA”-based aerials' powers and LEO-Sat's bandwidth resource allocation. Section 5 discusses the numerical simulations conducted, and Section 6 delivers the concluding remarks of this paper.

2. Related Work

In recent decades, aerial applications in wireless communications have attracted active research due to their maneuvering, flying, and hovering capabilities [2,3]. These functions enable their applications as flying BSs [21], forwarding communication links

from GBSs to remote users in non-rural areas [22], providing rescue services in post-disaster areas [5], strengthening communications in hotspot areas using aerial mounted reconfigurable intelligent surfaces (RISs) [6], etc.

On the other side, LEO-Sat has emerged as a promising technology for providing wireless communication services in recent years. These satellites orbit the Earth at a low altitude and can cover a relatively small area, allowing for high-speed, low-latency communication links. LEO-Sat systems are particularly attractive for applications such as sixth-generation (6G) networks, Internet of Things (IoT) connectivity, and other emerging wireless communication technologies. Regarding LEO-enabled wireless communications, in [8], a comprehensive overview of the physical and logical links, architectural and technological components needed to integrate LEO constellations into fifth generation (5G) and beyond 5G (B5G) systems was provided. In [10], a three-dimensional (3D) constellation optimization technique for a high-density LEO-based terrestrial–satellite communication model was proposed to optimize the number of satellites per constellation while attaining the minimum required backhaul per terminal. In [11], a load-balanced routing scheme was introduced to handle the LEO-Sat constellation framework. The work in [12] analyzed the downlink throughput of the LEO-Sat network that uses hopping spot beams. The authors presented upper and lower bounds on the downlink throughput based on the number of spot beams, interference restrictions, and coverage area. In [13], the authors discussed a user-centric handover methodology for ultra-dense LEO-Sat constellations to address the frequent handover problem and provide a higher quality of service. In [14], a low-complex massive multiple input multiple output (mMIMO) transmission technique with full frequency reuse (FFR) in LEO-Sat communication was proposed. The work of [15] investigated the joint optimization in LEO-Sat networks with multi-access edge computing servers to minimize the total delay of ground IoT devices.

Recently, a few researchers focused on integrating LEO-Sat and aerals to expand the coverage range. In [16], a multiplayer deep reinforcement learning (DRL) technique was utilized to optimize millimeter-wave (mmWave) and free-space optical (FSO) links of combined LEO-Sat and aerals. In [17], the authors suggested benefiting from aerals and LEO-Sat for information gathering in 6G networks. The focus was on minimizing the total energy cost while satisfying the data transmission demands, and the issue was solved using algorithms incorporating LEO-Sat-assisted aerial trajectory design. In [18], the authors leveraged LEO-Sat and aerals' caching for content delivery in ground systems to enhance connections and increase user capacity. The joint optimization problem of cache position, resource management, and aerial path was treated using an algorithm based on block coordinate descent and successive convex approximation methods. In [23], the authors of this paper considered the same problem of LEO-assisted aerial distribution but without considering the problem of jointly optimizing the LEO-Sat bandwidth and aerial TX power like the current work.

3. System Model

Figure 1 previews the under-investigation system model of integrating LEO-Sat and aerals to cover post-disaster regions where all nearby GBSs are destroyed or malfunctioned. The management and control (M&C) center orders the nearest survival GBS to the post-disaster area to manage the aerals' deployment assisted by LEO-Sat. To ensure that only one aerial covers a specific post-disaster location, the whole region is virtually divided into a number of clusters. These are depicted as dashed blue lines in Figure 1, with a total number of M clusters. Each cluster comprises K_i UD, $1 \leq i \leq M$. LEO-Sat facilitates communication between the closest survival GBS and aerals for both traffic and control data. Also, \mathcal{N} refers to the set of aerals, with a total number of N aerals, $N = 5$ in Figure 1, where $1 \leq j \leq N$ and $N < M$, are used to cover the post-disaster area. LEO-Sat continuously covers these aerals and can easily switch between satellites. The effects of this handover on network performance will be the subject of future investigations. At each time step t , the survival GBS determines which clusters the aerals should cover and assigns

them accordingly. This is then relayed to the aerials via LEO-Sat backhauling. Relaying and multi-hop transmissions among aerials are out of the scope of this paper and will be the subject of our future investigations. The goal is to properly allocate the aerials to clusters that maximize their attainable data rates while ensuring fair coverage based on UDs' densities in the distributed clusters. This allocation is subject to constraints such as the limited aerial battery budget and the limited LEO-Sat bandwidth resources. In the proposed system model, both rescue workers' and victims' devices are assumed to operate using the same frequency band for simplicity as the main focus is on the LEO-Sat assisted fair aerials distribution. However, we can assume that victims and rescue workers use two different communication bands to mitigate interference. In this case, aerials should be capable of using two different bands' interfaces, one for the workers and the other for the victims, which will complicate the aerials' communication task and put more burdens on their energy consumption. For sure, workers can communicate among themselves using device-to-device (D2D) communications, but they definitely need aerial connectivity to reach the ground monitoring/control center for management and control via LEO-Sat relaying. This interesting point will be a subject of our future investigations by using two different bands, one for workers and the other for victims, including its challenges and possible solutions. Also, this paper proposes a fully centralized scenario for aerial deployment carried out by the M&C center in the survival area, as shown in Figure 1. A decentralized scenario, where rescue workers control aerials deployment, will be the subject of our future investigations due to its numerous challenges, including the limited information on rescue workers, their limited battery capacities that cannot handle the complicated task of aerials deployment, the lack of connectivity to all aerials simultaneously, etc. In the following subsections, the link models of aerial-UD and LEO-aerial are described in detail, and the optimization problem is formulated.

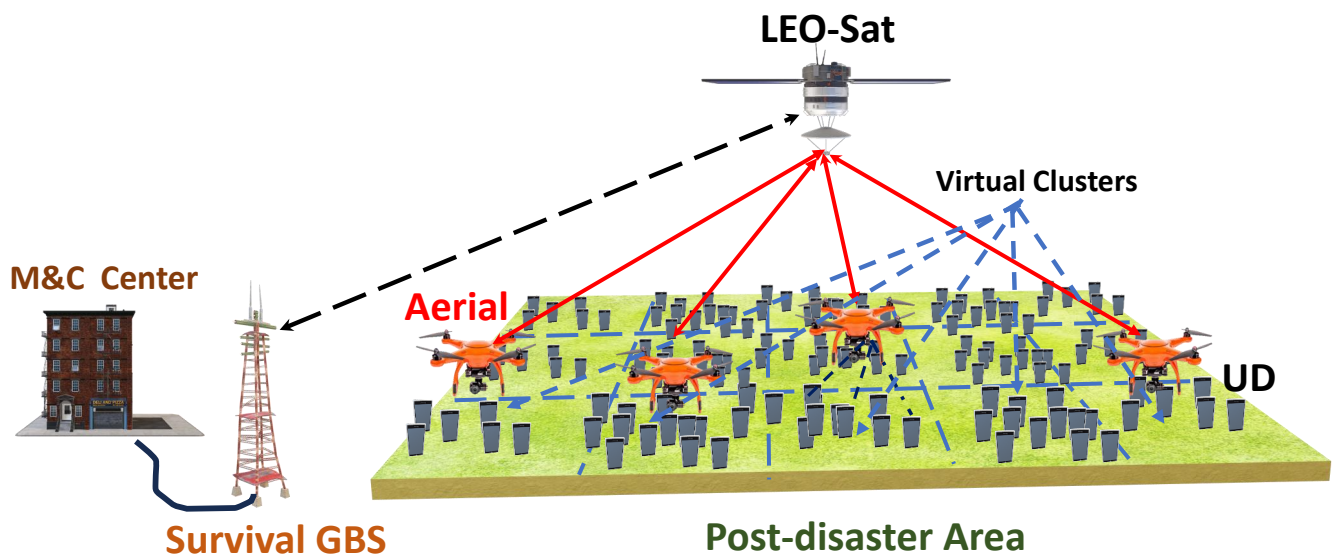


Figure 1. LEO-Sat and aerials integration in post-disaster scenario.

3.1. Aerial-UD Linkage Model

For aerial-UD communication linkage, we leveraged the model of [24], where the total path loss in dB between aerial j and UD k in cluster i can be expressed as follows:

$$\lambda_{jk_i}(d_{jk_i}) = \mathbb{P}^{LoS} \lambda_{jk_i}^{LoS}(d_{jk_i}) + \mathbb{P}^{NLoS} \lambda_{jk_i}^{NLoS}(d_{jk_i}) \tag{1}$$

where

$$\lambda_{jk_i}^{LoS}(d_{jk_i}) = 20 \log \left(\frac{4\pi f_V d_{jk_i}}{c} \right) + \rho^{LoS} \quad \& \quad \lambda_{jk_i}^{NLoS}(d_{jk_i}) = 20 \log \left(\frac{4\pi f_V d_{jk_i}}{c} \right) + \rho^{NLoS} \tag{2}$$

Herein, $\lambda_{jk_i}(d_{jk_i})$, is the total path loss. $\lambda_{jk_i}^{LoS}(d_{jk_i})$ and $\lambda_{jk_i}^{NLoS}(d_{jk_i})$ are the line of sight (LoS), and non-LoS (NLoS) components between aerial j and UD k in cluster i influenced by their related distance d_{jk_i} , respectively. Furthermore, f_V and c are the operating frequency of the aerial–UD link and the speed of light, respectively, where aerial is assumed to use the sub 6GHz wireless communication technology as given in [24]. ρ^{LoS} and ρ^{NLoS} indicate the LoS and NLoS losses in dB, respectively. \mathbb{P}^{LoS} and \mathbb{P}^{NLoS} , $\mathbb{P}^{NLoS} = 1 - \mathbb{P}^{LoS}$, define the LoS and NLoS linkage probabilities, mathematically modeled as [24].

$$\mathbb{P}^{LoS} = \left[1 + a \exp\left(-b\left(\varphi_{jk_i} - a\right)\right) \right]^{-1} \tag{3}$$

where a and b are the environmental constant parameters based on the ratio of built-up land area to the total land area, the mean number of buildings per unit area, and the buildings’ height distribution. Details of these parameters and how they affect the values of a and b can be found in [25]. φ_{jk_i} is the elevation angle between aerial j and UD k in cluster i , which is equal to $\varphi_{jk_i} = \tan^{-1}\left(\frac{h_j}{d_{Hjk_i}}\right)$, where h_j is the aerial j height and d_{Hjk_i} is the horizontal distance between aerial j and UD k within cluster i . An assumption is made that uplink transmissions from UDs in cluster i to aerial j , where the total data rate between them at time t can be formulated as:

$$\Psi_{j_i}(t) = B_V \sum_{k=1}^{K_i} \log_2 \left(1 + \frac{P_{rjk_i}(t)}{\sum_{u=1, u \neq k}^{K_i} P_{rju_i}(t) + \sigma^2} \right) \tag{4}$$

where B_V is the total available bandwidth for aerial j . $P_{rjk_i}(t)$ is the received power (RX) at aerial j from UD k in cluster i at time t determined by its TX power $P_{tk_{ij}}$ and $\lambda_{jk_i}(d_{jk_i}(t))$, where $d_{jk_i}(t)$ is the separation distance between them at time t . $\sum_{u=1, u \neq k}^{K_i} P_{rju_i}(t)$ is the sum of interfering RX powers at aerial j from other UDs in its covered cluster i , while σ^2 is the additive white Gaussian noise (AWGN) power. For further details about these link models and their related parameters, readers are advised to check [24].

3.2. LEO–Aerial Linkage Model

Herein, we leveraged the linkage model of [26], as the RX power at LEO-Sat from aerial j covering cluster i at time t , i.e., $P_{rSj_i}(t)$, is written as follows:

$$P_{rSj_i}(t) = \frac{P_{tj_iS}(t)cG_{tj_i}G_{rS}}{4\pi f_S d_{Sj_i}(t)} \tag{5}$$

Thus, the attainable data rate in bps can be formulated as:

$$\eta_{Sj_i}(t) = B_{Sj_i}(t) \log_2 \left(1 + \frac{P_{rSj_i}(t)}{\tau \varepsilon B_{Sj_i}(t)} \right), \tag{6}$$

In (5), $P_{tj_iS}(t)$ is the transmitted power from aerial to LEO-Sat at time t , and G_{tj_i} , G_{rS} are the transmitter and delivered antenna gains from aerial (LEO-Sat) to LEO-Sat (aerial), correspondingly. $d_{Sj_i}(t)$ defines the space between the LEO-Sat and aerial j covering cluster i . Also, f_S and c are the operating frequency of the LEO–aerial link and the speed of light, respectively, and LEO-Sat is assumed to use the sub 6GHz wireless communication technology as given in [26]. In (6), $B_{Sj_i}(t)$ is the allocated bandwidth of the LEO–aerial j link at time t , where it is assumed that the total LEO-Sat bandwidth B_{Smax} is divided among the available LEO-aerial links. Also, τ reflects the noise temperature, and ε is the Boltzmann constant.

3.3. Optimization Problem Formulation

The optimization problem aims to determine the best assignment vector $x_{ji}(t)$ for aerials-clusters at each time t , intending to maximize their long-term accumulative data rates. This objective should be accomplished while ensuring that cluster coverage is fair over the time horizon, given that $N < M$. The constrained resources of the aerials' batteries and LEO-Sat's bandwidth should also be considered. Mathematically, this optimization problem can be expressed in the following manner:

$$\begin{aligned} & \max_{x_{ji}(t), P_{tjS}(t), B_{Sj_i}(t)} \frac{1}{T} \sum_{t=1}^{T-1} \sum_{j=1}^N \sum_{i=1}^M x_{ji}(t) \min(\eta_{Sj_i}(t), \Psi_{j_i}(t)) \\ & \text{s.t} \\ & \text{C1 : } x_{ji}(t) \in \{0, 1\} \end{aligned} \tag{7a}$$

$$\text{C2 : } \sum_{j=1}^N \sum_{i=1}^M x_{ji}(t) \leq N \tag{7b}$$

$$\text{C3 : } \sum_{i=1}^M x_{ji}(t) = 1 \forall j \tag{7c}$$

$$\text{C4 : } x_{ji}(t) \Gamma_{j_i}(t) \leq \Gamma_{jR}(t) \forall j \tag{7d}$$

$$\text{C5 : } \frac{1}{T} \sum_{t=0}^{T-1} \sum_{j=1}^N x_{ji}(t) \geq \delta_i, \forall i \tag{7e}$$

$$\text{C6 : } \sum_{j=1}^N \sum_{i=1}^M x_{ji}(t) B_{Sj_i}(t) \leq B_{Smax} \tag{7f}$$

$$\text{C7 : } P_{tjS}(t) \leq P_{Vmax} \tag{7g}$$

where

$$\delta_i = \frac{K_i}{\sum_{i=1}^M K_i}, \tag{8}$$

$$\Gamma_{j_i}(t) = P_f T_{f_{j_i}}(t) + (P_h + P_{tjS}(t)) T_{h_{j_i}}, \tag{9}$$

where T is the time horizon, $x_{ji}(t) \in \{0, 1\}$ is an assignment binary indicator which equals one if cluster i is chosen to be covered by aerial j at time t otherwise zero. $\eta_{Sj_i}(t)$ given in (6) is the assigned capacity of the LEO-aerial link to cover cluster i by aerial j at time t . Also, $\Psi_{j_i}(t)$ given in (4) is the total data rate between aerial j and cluster i . In (7), the minimum of the aerial-UD link and the aerial-LEO link data rates is taken because UD data will be relayed to LEO-Sat via its coverage aerial. Thus, the total link speed between UD and LEO-Sat will be the minimum between both links as both will exist simultaneously. The constraint C2, which refers to the total number of chosen clusters, is less than or equal to N , i.e., the total number of aerials, as some aerials' batteries may run out of energy during the coverage and need re-charging. The third constraint, C3, reflects that at a time t , each aerial j covers only one cluster i . The fourth constraint, C4, refers to the energy consumption of aerial j , $\Gamma_{j_i}(t)$, needed to assist cluster i at time t should not overcome its remaining full battery capacity $\Gamma_{jR}(t)$ at time t . $\Gamma_{j_i}(t)$ is defined in (9), where it considers flying power P_f , hovering power P_h , and TX communication power $P_{tjS}(t)$. Both P_f and P_h are assumed to be constants. However, $P_{tjS}(t)$ is a function of time, and it should be optimized based on the current aerial j traffic need. $T_{f_{j_i}}(t)$ indicates the flying time of aerial j , which equals the division of the horizontal distance between its current position and target location in cluster i at time t , over the aerial speed. $T_{h_{j_i}}$ indicates the hovering time of aerial j over cluster i , which is assumed to be constant. The constraint C5 ensures fairness among clusters based on their UD densities, as given in (8). Constraint C6 means that the sum of the allocated LEO-aerial bandwidths should not exceed the maximum allowable bandwidth of

the LEO-Sat, i.e., B_{Smax} . Finally, constraint C7 indicates that the TX communication power of aerial at time t must not exceed its maximum allowable TX power P_{Vmax} .

4. Proposed CB-FBC and Genetic Approach

The prescribed problem in (7) is a non-linear dynamic time sequential programming lacking a closed-form optimal solution. To simplify it, we can take advantage of the fact that both $P_{tj_iS}(t)$ and $B_{Sj_i}(t)$ can be optimized based on the traffic needs of aerials after their deployment among the clusters. This allows us to divide this complex problem into two sub-problems. In the first one, we optimize the values of $x_{j_i}(t)$ while ensuring fairness in cluster coverage and considering the limited remaining energy of aerials. In the second sub-problem, the aerials' total data rates $\Psi_{j_i}(t)$ become fixed based on the optimized $x_{j_i}(t)$ values. Then, using these fixed values, we can optimize the values of $P_{tj_iS}(t)$ and $B_{Sj_i}(t)$. In the following, we propose the "CB-FBC" algorithm to address the first sub-problem, while a "GA" algorithmic approach addresses the second one.

4.1. Optimization of $x_{j_i}(t)$

Herein, the assignment vector $x_{j_i}(t)$ will be optimized under constraints C1 to C5. This sub-problem is a non-linear dynamic time sequential combinatorial optimization problem, where a group of clusters should be selected at each time t under the aforementioned constraints. Additionally, the M&C center has no information about this catastrophic area, including the number of survivors, their distributions, their traffic needs, etc. Such kinds of optimization problems cannot be solved using traditional optimization techniques as there is a lack of full information about the problem. More specifically, the values of $\Psi_{j_i}(t)$ are unknown for the optimizer itself. In these kinds of optimization problems, artificial intelligence by means of online learning provides a sufficient solution. This is due to the exploration and exploitation mechanism of online learning that can arrive at sufficient solutions without knowing the details of the problem. Thus, in this paper, this problem is modeled as a budget constraint combinatorial bandit with arms' fairness [27]. Generally, the MAB hypothesis is an efficient online learning methodology where a player intends to maximize his long-term reward via attempting the bandit's arms [19]. The player has no prior knowledge about arms except his observations about the played arms and their associated rewards. Within the bandit game, the player attempts to compromise between consistently exploiting the arm associated with the most considerable noticeable reward until now or exploring new ones [19]. In some MAB games, a cost should be paid for the played arms, which is subject to the player's limited budget. These types of MAB games are called budget-constrained MAB games [28]. Conversely, combinatorial bandits with arms' fairness given in [29] are bandits where the player chooses a group of arms named the super arm in each time step while guaranteeing long-term fairness in the arms' selection over time horizon. In this section, we will propose the "CB-FBC" algorithm to address the problem of $x_{j_i}(t)$ optimization. In this regard, the player will be the nearest survival GBS, the arms are the post-disaster clusters, and the reward is the sum of the aerials' data rates. The aerials' remaining battery capacity limits this game. Also, fairness should be maintained in post-disaster area clusters coverage based on their users' densities.

Algorithm 1 summarizes the envisioned "CB-FBC" algorithm, which will be implemented in the survival GBS as it is the bandit player. The algorithm inputs are the sets of all available post-disaster clusters and aerials, i.e., \mathcal{M} and \mathcal{N} , the initial values of users' densities δ_i , which are pre-estimated using GPS localization, and the design parameter Ω . The algorithm's output is the aerials-clusters assignment vector $x_{j_i}^*(t)$ at time t . For initialization, at $t = 0$, $w_i(t)$ which is the selection vector, $h_i(t)$ which is the number of times cluster i was drawn up to time t , $\hat{\gamma}_i(t)$ which is the mean data rate of cluster i up to time t , and $q_i(t)$ which is the queue of cluster i , are all initiated by zero $\forall i \in \mathcal{M}$. $q_i(t)$ assures fairness among the clusters, as discussed later. For $t = 1$ to T , the upper confidence bound (UCB) for $\forall i \in \mathcal{M}$ are set to $\tilde{\gamma}_i(t) = \hat{\gamma}_i(t-1) + \sqrt{(3 \log t)/(2h_i(t-1))}$ if $h_i(t-1) > 0$ or $\tilde{\gamma}_i(t) = 1$, if $h_i(t-1) \leq 0$. Then, $q_i(t)$ is estimated for $\forall i \in \mathcal{M}$ as illustrated in Algorithm 1.

At each trial t , the value of $q_i(t)$ is increased by δ_i and decreased by one if cluster i was drawn in time $t - 1$. Therefore, if cluster i is not chosen often, its $q_i(t)$ will be doubled by its UD density value, and vice versa. This prioritizes it for being drawn next time step. Hence, after estimating $q_i(t)$ and $\bar{\gamma}_i(t)$ for $\forall i \in \mathcal{M}$, a super arm $A(t) \subset \mathcal{M}$ is chosen according to the following criterion:

$$A(t) = \arg \max_{A(t) \subset \mathcal{M}} \sum_{i \in A(t)} (q_i(t) + \Omega \bar{\gamma}_i(t)), |A(t)| \leq N, \tag{10}$$

where Ω defines a design parameter that balances between choosing the cluster maximizes the achievable mean data rate or that maximizes fairness upon $q_i(t)$ values. $A(t)$ is evaluated by enumerating the $|A(t)|$ clusters having the highest $(q_i(t) + \Omega \bar{\gamma}_i(t))$. Afterward, the aerials should be distributed among them and attain $x_{j_i}^*(t)$ in a manner that minimizes aerials battery consumption subject to the aerial remaining battery energy at time t , i.e., $\Gamma_{jR}(t)$, as given in constraint C4 in(7). To do that, $\Gamma_{j_i}(t)$ matrix is evaluated for $\forall i \in A(t)$ and $\forall j \in \mathcal{N}$ using (9) by assuming the worst case scenario when $P_{tj_iS}(t) = P_{Vmax}$ for $\forall j \in \mathcal{N}$. If the $\min(\Gamma_{j_i}(t)) < \Gamma_{jR}(t)$ for any aerial j , it should fly back for re-charging its battery; otherwise it will fly towards cluster i to cover it and then $x_{j_i}^*(t)$ is set to 1. Afterwards, this cluster will be removed from $A(t)$ by putting $\Gamma_{j_i}(t) = \infty$ for $\forall j \in \mathcal{N}$. Then, $\Gamma_{jR}(t + 1)$ are updated for the next time step based on the energy consumed by aerials or that re-charged. Finally, the mean data rates related to the chosen $A(t)$ are noticed, and its associated parameters are updated as stated in Algorithm 1, including updating the value of δ_i based on aerials real observations about users' densities in $A(t)$.

4.2. Optimization of $P_{tj_iS}(t)$ and $B_{Sj_i}(t)$

After obtaining the values of $x_{j_i}^*(t)$ and distributing the aerials among the selected $A(t)$, the values of $\Psi_{j_i}(t)$ become known. Then, in the next step, the values of $P_{tj_iS}(t)$ and $B_{Sj_i}(t)$ should be optimized to accommodate the values of $\Psi_{j_i}(t)$ related to every aerial under constraints C6 and C7 in (7). This optimization problem can be formulated as follows:

$$\begin{aligned} & \max_{P_{tj_iS}(t), B_{Sj_i}(t)} \frac{1}{T} \sum_{t=1}^{T-1} \sum_{j=1}^N \min(\eta_{Sj_i}(t), \Psi_{j_i}(t)) \\ & \text{s.t} \\ & \text{C6 : } \sum_{j=1}^N B_{Sj_i}(t) \leq B_{Smax} \end{aligned} \tag{11a}$$

$$\text{C7 : } P_{tj_iS}(t) \leq P_{Vmax} \tag{11b}$$

This optimization problem can be further simplified by reformulating it as minimizing the absolute difference between $\eta_{Sj_i}(t)$ and $\Psi_{j_i}(t)$ via optimizing the control parameters $P_{tj_iS}(t)$ and $B_{Sj_i}(t)$, which can be written as follows:

$$\begin{aligned} & \min_{P_{tj_iS}(t), B_{Sj_i}(t)} \sum_{j=1}^N \text{abs}|\eta_{Sj_i}(t) - \Psi_{j_i}(t)| \\ & \text{s.t} \\ & \text{C1 : } \sum_{j=1}^N B_{Sj_i}(t) \leq B_{Smax} \end{aligned} \tag{12a}$$

$$\text{C2 : } P_{tj_iS}(t) \leq P_{Vmax} \tag{12b}$$

This problem is non-linear programming due to the absolute function. Actually, various optimization techniques can handle this optimization problem, including GA, sequential quadratic programming (SQP), particle swarm optimization (PSO), interior point optimization, Bayesian optimization, etc. In this paper, we used the GA because it is well-suited for

problems with non-linear objective functions like the one given above. The GA operators (crossover and mutation) allow for effective exploration in complex and non-linear spaces. Also, the GA can handle constraints effectively using penalty functions or specialized constraint-handling mechanisms. This is important in the constrained optimization problem like the one given above where $P_{tj_i S}(t)$ must not exceed P_{Vmax} and $B_{Sj_i}(t)$ must not exceed B_{Smax} . Thus, the penalty function provided by the GA is best suited to this scenario. Finally, the GA's population-based approach can help prevent premature convergence to suboptimal solutions. It allows for the simultaneous exploration of multiple candidate solutions, increasing the algorithm's robustness. The comparisons with other candidate optimizers to find the best one are out of the scope of this paper, and they will be the subject of our future investigations. In this paper, a "GA" algorithmic approach is used to address (11b) within its constraints. The inputs to the "GA" algorithm are the values of $\Psi_{j_i}(t)$, B_{Smax} , P_{Vmax} in addition to the adjusting parameters of the "GA" algorithm such as the population size P_s , the maximum number of generations G_e , the percentage of mutation ϵ_m , and the percentage of crossover ϵ_c . The fitness function will be:

$$Fit(t) = \sum_{j=1}^N \text{abs}|\eta_{Sj_i}(t) - \Psi_{j_i}(t)| \tag{13}$$

Algorithm 1: Proposed CB-FBC Algorithm implemented in GBS

Output: $x_{j_i}^*(t)$
Input: \mathcal{M}, \mathcal{N} , initiated δ_i using GPS localization, and Ω .
Initialization: At $t = 0$, $w_i(t) = 0$, $h_i(t) = 0$, $\hat{\gamma}_i(t) = 0$, and $q_i(t) = 0 \forall i \in \mathcal{M}$.

```

1 for  $t = 1, 2, \dots, T$  do
2   for  $i = 1, 2, \dots, M$  do
3     if  $h_i(t-1) > 0$  then
4        $\tilde{\gamma}_i(t) = \hat{\gamma}_i(t-1) + \sqrt{(3 \log t) / (2h_i(t-1))}$ 
5     end
6     else
7        $\tilde{\gamma}_i(t) = 1$ 
8     end
9   end
10   $q_i(t) = \max\{q_i(t-1) + \delta_i - w_i(t-1), 0\}$ 
    • choose the super arm  $A(t)$  that achieves:
       $A(t) = \arg \max_{A(t) \subset \mathcal{M}} \sum_{i \in A(t)} (q_i(t) + \Omega \tilde{\gamma}_i(t))$ ,  $|A(t)| \leq N$ 
    • Select  $d_{j_i}^*(t)$  that minimizes aerials energy consumptions as:
      1. Calculate  $\Gamma_{j_i}(t)$  matrix  $\forall i \in A(t)$  and  $\forall j \in \mathcal{N}$  using (9) assuming  $P_{tj_i S}(t) = P_{Vmax}$ 
      2. Recharge aerial  $j$  or connect it with cluster  $i$ 
      as follows:
      for  $j = 1 : N$  do
        if  $\min(\Gamma_{j_i}(t)) < \Gamma_{jR}(t)$  then
          | aerial  $j$  flies back for recharging
        end
        else
          if  $\min(\Gamma_{j_i}(t)) \geq \Gamma_{jR}(t)$  then
            a.  $\{i, j\} = \arg \min(\Gamma_{j_i}(t))$ 
            b.  $x_{j_i}^*(t) = 1$ 
            c.  $\Gamma_{j_i}(t) = \infty \forall j \in \mathcal{N}$ 
            d. Update  $\Gamma_{jR}(t+1) \forall j \in \mathcal{N}$ 
          end
        end
      end
    • Collect data rates associated with the drawn super arm  $A(t)$  then
      update its corresponding parameters:
      1.  $w_i(t) = 1 \forall i \in A(t)$ .
      2.  $h_i(t) = h_i(t-1) + 1 \forall i \in A(t)$ 
      3.  $\hat{\gamma}_i(t) = \frac{1}{h_i(t)} \sum_{y=1}^{h_i(t)} w_i(y) \Psi_{j_i}(y) \forall i \in A(t)$ 
      4. Update  $\delta_i \forall i \in A(t)$ 
11 end

```

The output of the “GA” algorithm is the sub-optimum values $P_{tj_iS}^*(t)$ and $B_{Sj_i}^*(t)$ as detailed in Algorithm 2. At the beginning of the algorithm, the population “Pop” of $P_{tj_iS}(t)$ and $B_{Sj_i}(t) \forall N$ is constructed randomly in the range of $[0, P_{Vmax}]$ and $[0, B_{Smax}]$, respectively, with a size of P_s . Then, for $1 \leq g \leq G_e$, the fitness function is evaluated for all members in “Pop”, and the member characterized with the highest fitness value is selected. The parents, “Parents”, of size P_a are selected from “Pop” based on the calculated fitness function values. Then, a percentage of parents are crossed over to produce the children, which after mutation produces the new population, “NewPop”. The generated “NewPop” are used to refine the selections of $P_{tj_iS}^*(t)$ and $B_{Sj_i}^*(t)$ in the next iteration as given in Algorithm 2. This algorithm is also implemented in the terrestrial GBS as it is the most energized component in the network. Then, the adjusted values of $P_{tj_iS}^*(t)$ and $B_{Sj_i}^*(t)$ are sent via control signals to LEO-Sat to adjust its bandwidth values and then relay the adjusted $P_{tj_iS}^*(t)$ values to the aeriels.

Algorithm 2: Proposed GA implemented in GBS

Output: $P_{tj_iS}^*(t), B_{Sj_i}^*(t)$
Input: $\Psi_{j_i}(t), P_s, G_e, \epsilon_m, \epsilon_c, B_{Smax}, P_{Vmax}$, and Fit .
Initialization: Construct the population Pop of size P_s by randomly selecting P_s values of $P_{tj_iS}(t)$ in the range of $[0, P_{Vmax}]$, and $B_{Sj_i}(t)$ in the range of $[0, B_{Smax}]$ for $\forall j \in N$.

```

1 for  $g = 1, 2, 3 \dots, G_e$  do
    • Evaluate:  $Fit_k(t), k \in P_s$  in  $Pop$  using (16)
    • Calculate:  $\{P_{tj_iS}^*(t), B_{Sj_i}^*(t)\} = \max_{\forall k \in P_s} \{Fit_k(t)\}$ 
    • Select: the set of  $Parents$  of size  $P_a$  from  $Pop$  using Roulette Wheel, Tournament based on the values of  $Fit_k(t)$ 
    • Set:  $NewPop = \{\}$ 
    • Crossover:
    • for  $i = 1, 2 \dots, \frac{P_a}{2}$  do
         $Parent1 = Parents(2i - 1)$ 
         $Parent2 = Parents(2i)$ 
        if  $rand < \epsilon_c$  then
            |  $\{Child1, Child2\} = \text{Crossover}\{Parent1, Parent2\}$ 
        end
        else
            |  $\{Child1, Child2\} = \{Parent1, Parent2\}$ 
        end
        end
         $NewPop = \{NewPop, Child1, Child2\}$ 
    • Mutation:
    • for  $\forall Child \in NewPop$  do
        if  $rand < \epsilon_m$  then
            | Mutate  $Child$  and update it in  $NewPop$ 
        end
        end
        Replace  $Pop$  by  $newPop$ 
2 end
  
```

5. Numerical Analysis

This section utilizes Monte-Carlo (MC) simulations to demonstrate the efficiency of the envisioned “CB-FBC” and “GA” algorithms approach. The studied post-disaster is 1 Km², divided into 36 clusters containing a random number of users/survivors. The LEO-Sat altitude is 550 Km, while the aerial altitude is 100 m. An assumption is made that

the nearest terrestrial GBS has full connectivity with the LEO-Sat, and all aerials are within full coverage of the LEO-Sat. The handover process between the LEO-Sat and both GBS and aerials can be conducted smoothly, and its impact on network performance will be investigated in future studies. The total bandwidth allocated for the aerial is 40 MHz, and for the LEO-Sat, it is 100 MHz. For the “GA” algorithm, the number of populations is 20, the maximum number of generations is 50, the percentage of mutation is 0.3, the percentage of crossover is 0.3, and the percentage of creation function is 0.1. Other simulation parameters are provided in Table 1. For performance comparisons, we compare the proposed approach with a basic UCB MAB algorithm given in [19] for cluster selection. Also, the GA is used for the aerials’ TX power and LEO-Sat bandwidth optimization for fair comparisons. In the UCB-based clusters selection, the clusters that maximize the upper confidence criterion are selected by the survival GBS for aerial deployment without any fairness guarantee, where the super arm selection is carried out based on the following equation [19]:

$$A(t) = \arg \max_{A(t) \subset \mathcal{M}} \sum_{i \in A(t)} \left(\bar{\gamma}_i(t) + \sqrt{\frac{2 \ln(t)}{h_i(t)}} \right), |A(t)| \leq N, \quad (14)$$

where $A(t)$ is the group of selected clusters, \mathcal{M} is the space of all available clusters, $h_i(t)$ is the number of times cluster i was selected just before time t , and $\bar{\gamma}_i(t)$ is the average data rate of cluster i just before time t . Also, naïve benchmarks like nearest and random approaches are involved in the comparisons. In the “Nearest” approach, the aerials always select their nearest clusters without collisions, i.e., no aerials cover the same cluster. If the same cluster is the nearest for two or more aerials, it will be covered by the nearest one of them. The other aerials will cover their second or third nearer cluster, and so on. Also, aerials operate at their maximum TX power values, i.e., P_{Vmax} , while the LEO-Sat bandwidth is equally allocated between the LEO–aerial links. Regarding the “Rand” approach, the clusters are selected randomly, the aerials operate at their maximum TX powers, and the LEO-Sat bandwidth is randomly allocated within the LEO–aerial links.

Table 1. Simulation parameters.

Parameter	Value
B_{Smax}, B_V	100 MHz [26], 40 MHz [24]
P_{tjk_i}, P_{Vmax}	1 Watt, 10 Watt [26]
K_i	Uniformly random in the range [1, 100]
f_V, f_S	2 GHz [24], 2.4 GHz [26]
$\sigma^2 (dBm)$	$-174 + 10 \log_{10}(W) + 10$ [30]
P_f, P_h	4, 2 Watt [31]
τ and ϵ	1000 and 1.38×10^{-23} [26]
ρ^{LOS} and ρ^{NLOS}	0.1 dB and 21 dB [24]
UD data load	5 Gbit
T, Ω	1000, 0.01
G_{tj_i}, G_{rS}	15 dB [26]
a, b	4.88, 0.429 [24]

5.1. Performance Analysis

Figure 2 adjusts the number of GA generations, where the average total system rate is evaluated against different numbers of GA generations ranging from 10 to 100. In this simulation, the number of aerials is set to 14 to cover 36 clusters. From this figure, as the number of generations increases from 10 to 50, the average total system rate increases by 28%, while it only increases by 4% when increasing the number of generations from

50 to 100. This means that the average total system rate starts to saturate after 50 number of generations. Considering that the complexity of the GA algorithm increases linearly with an increase in the number of generations, we selected 50 generations to trade off complexity and performance as aforementioned.

Figure 3 displays the average total system rate versus distinct numbers of aeriels. As the number of aeriels increases, so does the mean total system rate for all compared schemes due to a greater coverage area. However, the proposed approach, named “CB-FBC” and the “GA” algorithms yield a higher mean total system rate than the other benchmark schemes. This is due to their ability to efficiently distribute the aeriels across post-disaster clusters while maximizing their sum rates. Moreover, the total system rate of the proposed approach is higher than that of the basic “UCB+GA” MAB algorithm. This is because the proposed CB-FBC algorithm balances between the achievable data rate and the clusters’ selection fairness, while UCB only maximizes the confidence of the selected clusters. It is also noteworthy that the “Nearest” algorithm outperforms the “Rand” algorithm in mean sum rate performance because it equally distributes LEO-Sat bandwidth among the aeriels, whereas in the “Rand” scheme, they are allocated randomly. Also, Figure 3 illustrates that the proposed approach outperforms the “UCB+GA”, “Nearest”, and “Rand” methods by 1.168, 1.33 and 1.55 at $N = 2$, correspondingly. At $N = 14$, the proposed approach outperforms them by 1.14, 1.32, and 2 times, respectively.

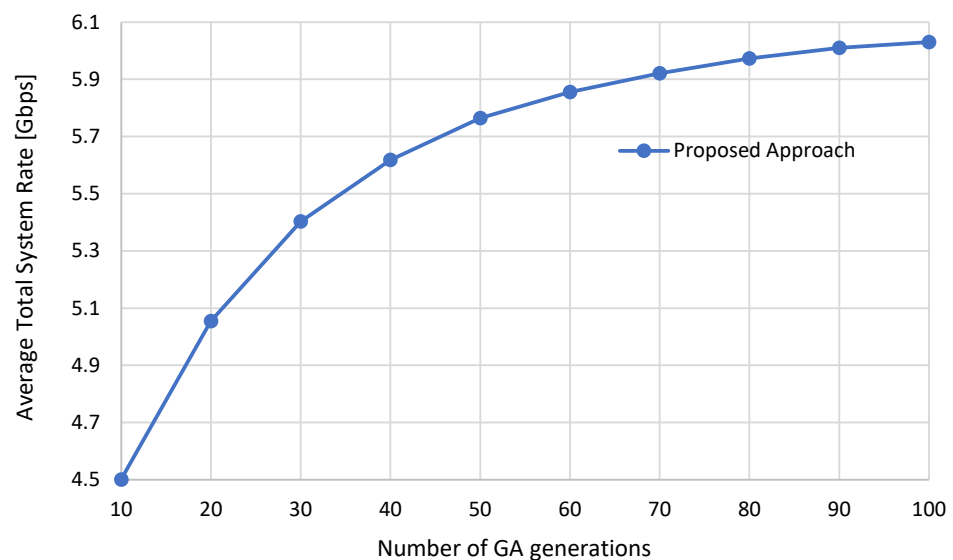


Figure 2. Total system rate against the number of GA generations.

Figure 4 depicts the sum of the aeriels’ energy consumption in KJ. As the number of aeriels increases, so does the sum of the aeriels’ energy consumption for all compared schemes. However, due to the proposed approach’s awareness of the limited aerial battery budget and optimization of aerial TX power, it demonstrates superior performance over other benchmarks regarding aerial energy consumption. The proposed approach has lower aerial energy consumptions than the “UCB+GA” algorithm because it optimizes the flying, hovering, and TX powers of the aeriels while UCB only optimizes the aeriels’ TX powers using the GA algorithm. Moreover, the “Nearest” algorithm shows a better aerial energy consumption achievement than the “Rand” algorithm as it always chooses the clusters nearest to the aeriels, which significantly reduces their flying energy consumption. On the other hand, in the “Rand” approach, clusters are randomly selected, which increases their flying energy consumption relative to the “Nearest” algorithm. This is the reason why the “Rand” algorithm has the worst aerial energy consumption performance. Although both the proposed approach and the “Nearest” algorithm almost select the nearest cluster, the proposed approach has lower energy consumption. This is because the proposed approach optimizes the aeriels’ TX communication powers using “GA” algorithms, while

the “Nearest” approach uses fixed maximum TX power allocation. When the number of aerials is low, e.g., $N = 2$, the proposed approach has a lower sum of the aerials’ energy consumption than “UCB+GA”, the “Nearest” and “Rand” schemes by 5.2%, 42.7%, and 51.88%, respectively. However, for many aerials, e.g., $N = 14$, these values become 19.23%, 40.7%, and 71.97%, respectively. Compared to the scheme proposed in [23], the improvements over “Rand” and “Nearest” schemes were only 7% and 5%, respectively, at $N = 14$ without any improvements at $N = 2$. This superior energy consumption performance of the proposed scheme over that proposed in [23] comes from the aerial TX power optimization mechanism provided by the proposed “GA” algorithm, where the scheme proposed in [23] has no such functionality.

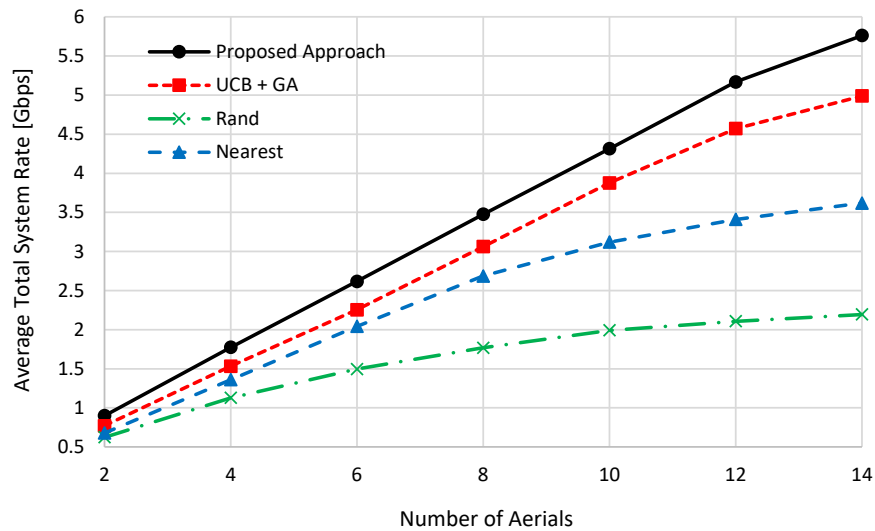


Figure 3. Total system rate against the numbers of aerials.

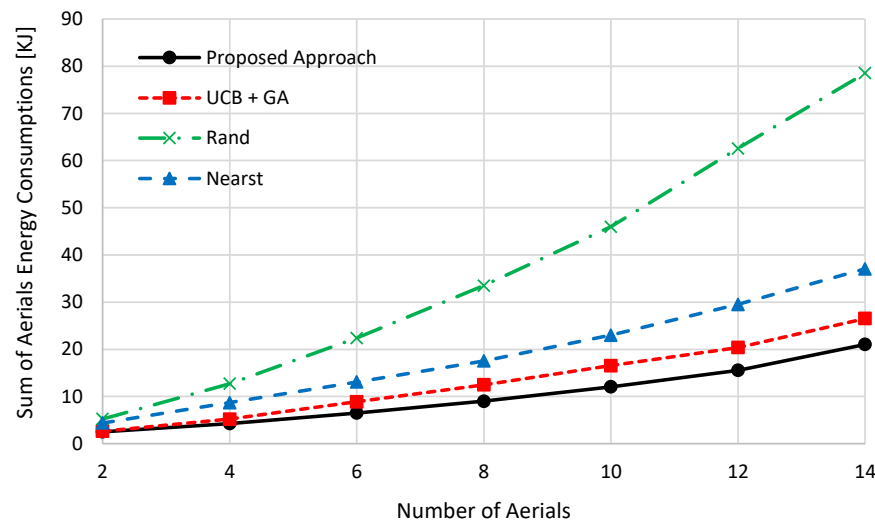


Figure 4. Sum of aerials energy consumption against the number of aerials.

Figure 5 gives the clusters selection fairness index, which is calculated as:

$$\chi = \sum_{i=1}^M \text{abs} \left| \frac{h_i(T)}{\sum_{i=1}^M h_i(T)} - \delta_i \right| \tag{15}$$

where the term $\frac{h_i(T)}{\sum_{i=1}^M h_i(T)}$ defines how many times cluster i was chosen over the time horizon T divided by the total number of clusters selected. If the clusters were drawn upon their

user densities, δ_i , χ reaches zero. This means that as the value of χ becomes smaller, better fairness is maintained in the clusters' coverage. From Figure 5, the proposed approach has the lowest χ values at all tested number of aerials. The clusters' fairness index of the "UCB-GA" algorithm is higher than that of the proposed approach because it has no fairness functionality. As the clusters are randomly selected in the "Rand" selection approach, the χ value is almost constant irrespective of the number of aerials used, because the term $\left(\frac{h_i(T)}{\sum_{i=1}^M h_i(T)}\right)$ almost has the same value for $\forall i$, which is almost equal to $1/M$. On the other hand, both "UCB+GA" and the "Nearest" approaches have the worst fairness performance among the schemes involved in the comparisons because aerials always select their high confidence or nearest clusters, which causes unfairness in cluster coverage. Moreover, as the number of aerials increases, the χ values of both schemes are decreased, enhancing their fairness performance. This is because many clusters are selected at each time step, which induces better fairness performance over time horizon. As the number of aerials increments, the χ of all schemes tends to approach that of the "Rand" selection. This is due to the limited number of clusters accessible for choice at every trial, and as the number of aerials is equal to the number of clusters; all schemes will merge to the same point of "Rand" selection. From Figure 4, at $N = 2$, the clusters selection fairness index of the proposed scheme is lower than that corresponding to "UAB+GA", "Nearest", and "Rand" selections by 98.5%, 98.57%, and 95.83%, respectively. However, at $N = 14$, these values become 73.21%, 74.64%, and 50.7%, respectively.

Figure 6 displays the ratio of LEO-Sat bandwidth utilization for various schemes. The "Nearest" algorithm fully utilizes the LEO-Sat bandwidth since it distributes it equally among the LEO-aerial links. As shown in Figure 6, its bandwidth utilization ratio equals 1. On the other hand, the "Rand" scheme's bandwidth utilization ratio is nearly equal to 0.5 since the bandwidth of each LEO-aerial link is randomly assigned from the range $[1, B_{Smax}/N]$. As the proposed approach and "UCB-GA" algorithms optimize the allocated LEO-Sat bandwidth according to the aerials' traffic requirements using GA, they have the same performance that comes from utilizing the LEO-Sat bandwidth most efficiently. Initially, they achieve a low Sat bandwidth utilization ratio at fewer aerials. However, full Sat bandwidth utilization occurs as the number of aerials increases. This results from aerials' high total traffic demands, which operate the LEO-Sat at its maximum capacity. At $N = 2$, they have a lower SAT bandwidth utilization ratio than the "Nearest" and "Rand" approaches by 82%.

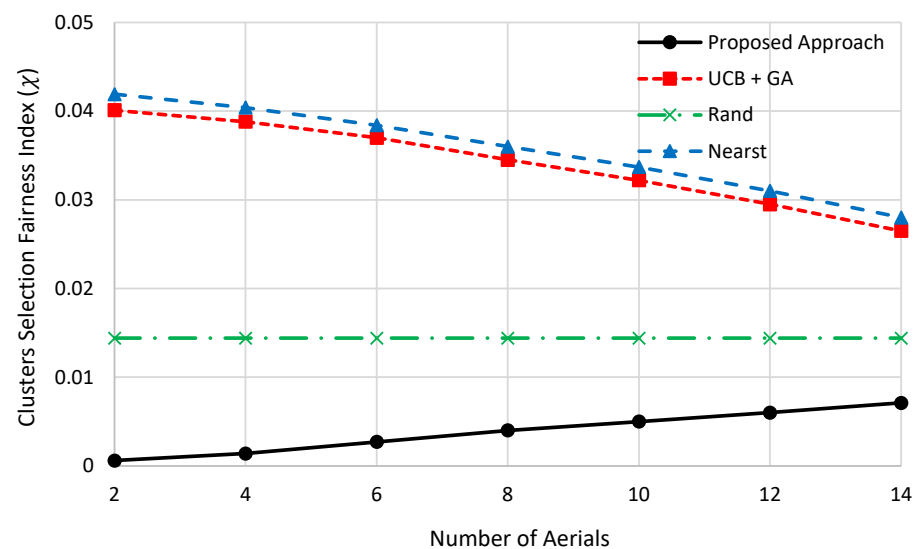


Figure 5. Clusters selection fairness index against the number of aerials.

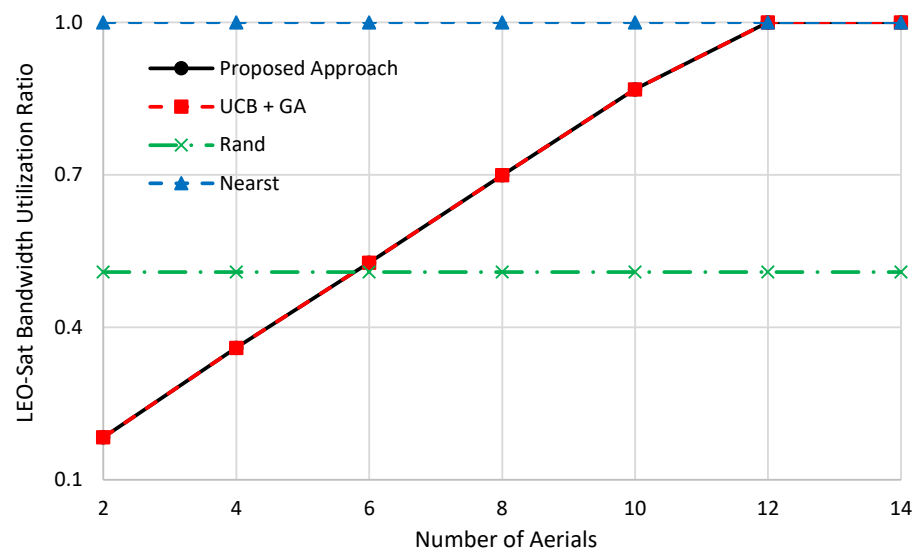


Figure 6. LEO-SAT bandwidth utilization ratio against the numbers of aerials.

5.2. Computational Complexity Analysis

The main computational complexity of the proposed approach issues from the proposed “CB-FBC” and the “GA” algorithms. The computational complexity of the envisioned “CB-FBC” algorithm is equal to $\mathcal{O}(N^2) + \mathcal{O}(N + 1)$, where $\mathcal{O}(N^2)$ comes from minimizing energy consumption and $\mathcal{O}(N + 1)$ from the sorting operation and updating the parameters of the selected super arm. The computational complexity of a “GA” algorithm is influenced by several factors, such as the population size, the number of generations, the objective function complexity, and “GA” algorithm functions such as mutation, crossover, and selection. Generally, this can be expressed as follows [32]:

$$\text{Complexity of GA} = \mathcal{O}(nGP(C + UOS)) \quad (16)$$

where n is the number of decision variables that is equal to $2N$ in the proposed “GA” algorithm. G and P are the number of maximum generations and the population size, which are set to 50 and 20, respectively. C is the computational complexity of the fitness function given in (16) which is equal to $\mathcal{O}(2N)$. U , O , and S are the computational complexities of the mutation, crossover, and selection functions used by the “GA” algorithm. For simplicity, we can ignore the effect of “GA” algorithm functions as they typically have constant complexity and are lower than the fitness function complexity. Thus, the computational complexity of the envisioned “GA” algorithm equals $\mathcal{O}(4000N^2)$. To sum up, the total computational complexity of the proposed approach, i.e., “CB-FP” + “GA” algorithms, will be in the range of $\mathcal{O}(N^2)$.

Thus, the improved performance of the proposed approach over the naïve algorithms and that proposed in [23] comes with a slight increase in its computational complexity. However, as the algorithm will be run on the power supply feed terrestrial GBS, this will not be a big issue for the proposed approach.

6. Conclusions

In summary, this study suggests a new approach for aerials’ deployment in post-disaster areas using LEO-Sat assistance, aiming to maximize the accessible sum rate of aerials simultaneously with achieving fairness in cluster coverage based on UDs’ densities and considering the finite existing resources of both LEO-Sat and aerials. The approach utilizes the “CB-FBC” algorithm to distribute aerials eventually while considering fairness in the clusters’ coverage and the aerials’ battery capacity. A “GA” was also used to optimize the allocation of aerials’ TX powers and LEO-Sat’s bandwidths. The study conducted extensive numerical analysis, which shows that the proposed approach outperforms naïve

benchmark schemes like nearest- and random-based selections regarding total system rate, aerials' batteries' consumption, aerials' TX powers allocation, and LEO-Sat bandwidth utilization. Overall, this study opens opportunities for using LEO–aerial integration in different 6G network scenarios.

Author Contributions: All authors contributed equally to this paper. All authors have read and agreed to the published version of the manuscript.

Funding: The authors extend their appreciation to Prince Sattam Bin Abdulaziz University for funding this research work through the project number (PSAU/2023/01/24766).

Data Availability Statement: Data are available upon request to the authors.

Conflicts of Interest: The authors declare no conflict of interest.

References

1. Hashesh, A.O.; Hashima, S.; Zaki, R.M.; Fouda, M.M.; Hatano, K.; Eldien, A.S.T. AI-Enabled UAV Communications: Challenges and Future Directions. *IEEE Access* **2022**, *10*, 92048–92066. [\[CrossRef\]](#)
2. Mozaffari, M.; Saad, W.; Bennis, M.; Nam, Y.H.; Debbah, M. A Tutorial on UAVs for Wireless Networks: Applications, Challenges, and Open Problems. *IEEE Commun. Surv. Tutor.* **2019**, *21*, 2334–2360. [\[CrossRef\]](#)
3. Nomikos, N.; Gkonis, P.K.; Bithas, P.S.; Trakadas, P. A Survey on UAV-Aided Maritime Communications: Deployment Considerations, Applications, and Future Challenges. *IEEE Open J. Commun. Soc.* **2023**, *4*, 56–78. [\[CrossRef\]](#)
4. Zhang, S.; Liu, J. Analysis and Optimization of Multiple Unmanned Aerial Vehicle-Assisted Communications in Post-Disaster Areas. *IEEE Trans. Veh. Technol.* **2018**, *67*, 12049–12060. [\[CrossRef\]](#)
5. Hashima, S.; Hatano, K.; Mohamed, E.M. Multiagent Multi-Armed Bandit Schemes for Gateway Selection in UAV Networks. In Proceedings of the 2020 IEEE Globecom Workshops (GC Workshops), Taipei, Taiwan, 7–11 December 2020; pp. 1–6.
6. Mohamed, E.M.; Hashima, S.; Hatano, K. Energy Aware Multiarmed Bandit for Millimeter Wave-Based UAV Mounted RIS Networks. *IEEE Wirel. Commun. Lett.* **2022**, *11*, 1293–1297. [\[CrossRef\]](#)
7. Guo, F.; Lu, L.; Zang, Z.; Shikh-Bahaei, M. Machine Learning for Predictive Deployment of UAVs With Multiple Access. *IEEE Open J. Commun. Soc.* **2023**, *4*, 908–921. [\[CrossRef\]](#)
8. Leyva-Mayorga, I.; Soret, B.; Röper, M.; Wübber, D.; Matthiesen, B.; Dekorsy, A.; Popovski, P. LEO Small-Satellite Constellations for 5G and Beyond-5G Communications. *IEEE Access* **2020**, *8*, 184955–184964. [\[CrossRef\]](#)
9. Elhalawany, B.M.; Gamal, C.; Elsayed, A.; Elsherbini, M.M.; Fouda, M.M.; Ali, N. Outage Analysis of Coordinated NOMA Transmission for LEO Satellite Constellations. *IEEE Open J. Commun. Soc.* **2022**, *3*, 2195–2202. [\[CrossRef\]](#)
10. Deng, R.; Di, B.; Zhang, H.; Kuang, L.; Song, L. Ultra-Dense LEO Satellite Constellations: How Many LEO Satellites Do We Need? *IEEE Trans. Wirel. Commun.* **2021**, *20*, 4843–4857. [\[CrossRef\]](#)
11. Dong, C.; Xu, X.; Liu, A.; Liang, X. Load balancing routing algorithm based on extended link states in LEO constellation network. *China Commun.* **2022**, *19*, 247–260. [\[CrossRef\]](#)
12. Mokhtar, A.; Azizoglu, M. On the downlink throughput of a broadband LEO satellite network with hopping beams. *IEEE Commun. Lett.* **2000**, *4*, 390–393. [\[CrossRef\]](#)
13. Li, J.; Xue, K.; Liu, J.; Zhang, Y. A User-Centric Handover Scheme for Ultra-Dense LEO Satellite Networks. *IEEE Wirel. Commun. Lett.* **2020**, *9*, 1904–1908. [\[CrossRef\]](#)
14. You, L.; Li, K.X.; Wang, J.; Gao, X.; Xia, X.G.; Ottersten, B. Massive MIMO Transmission for LEO Satellite Communications. *IEEE J. Sel. Areas Commun.* **2020**, *38*, 1851–1865. [\[CrossRef\]](#)
15. Hao, Y.; Song, Z.; Zheng, Z.; Zhang, Q.; Miao, Z. Joint Communication, Computing, and Caching Resource Allocation in LEO Satellite MEC Networks. *IEEE Access* **2023**, *11*, 6708–6716. [\[CrossRef\]](#)
16. Singya, P.K.; Alouini, M.S. Performance of UAV-Assisted Multiuser Terrestrial-Satellite Communication System over Mixed FSO/RF Channels. *IEEE Trans. Aerosp. Electron. Syst.* **2022**, *58*, 781–796. [\[CrossRef\]](#)
17. Ma, T.; Zhou, H.; Qian, B.; Cheng, N.; Shen, X.; Chen, X.; Bai, B. UAV-LEO Integrated Backbone: A Ubiquitous Data Collection Approach for B5G Internet of Remote Things Networks. *IEEE J. Sel. Areas Commun.* **2021**, *39*, 3491–3505. [\[CrossRef\]](#)
18. Tran, D.H.; Chatzinotas, S.; Ottersten, B. Satellite- and Cache-Assisted UAV: A Joint Cache Placement, Resource Allocation, and Trajectory Optimization for 6G Aerial Networks. *IEEE Open J. Veh. Technol.* **2022**, *3*, 40–54. [\[CrossRef\]](#)
19. Auer, P.; Cesa-Bianchi, N.; Fischer, P. Finite-time Analysis of the Multiarmed Bandit Problem. *Mach. Learn.* **2002**, *47*, 235–256. [\[CrossRef\]](#)
20. Holland, J.H. Genetic Algorithms. *Sci. Am.* **1992**, *267*, 66–73. [\[CrossRef\]](#)
21. Huang, H.; Savkin, A.V. Deployment of Heterogeneous UAV Base Stations for Optimal Quality of Coverage. *IEEE Internet Things J.* **2022**, *9*, 16429–16437. [\[CrossRef\]](#)
22. Ahmed, S.; Chowdhury, M.Z.; Jang, Y.M. Energy-Efficient UAV Relaying Communications to Serve Ground Nodes. *IEEE Commun. Lett.* **2020**, *24*, 849–852. [\[CrossRef\]](#)

23. Mohamed, E.M. LEO satellite assisted UAV distribution using combinatorial bandit with fairness and budget constraints. *PLoS ONE* **2023**, *18*, e0290432. [[CrossRef](#)]
24. Sabzehali, J.; Shah, V.K.; Fan, Q.; Choudhury, B.; Liu, L.; Reed, J.H. Optimizing Number, Placement, and Backhaul Connectivity of Multi-UAV Networks. *IEEE Internet Things J.* **2022**, *9*, 21548–21560. [[CrossRef](#)]
25. Al-Hourani, A.; Kandeepan, S.; Lardner, S. Optimal LAP Altitude for Maximum Coverage. *IEEE Wirel. Commun. Lett.* **2014**, *3*, 569–572. [[CrossRef](#)]
26. Jia, Z.; Sheng, M.; Li, J.; Niyato, D.; Han, Z. LEO-Satellite-Assisted UAV: Joint Trajectory and Data Collection for Internet of Remote Things in 6G Aerial Access Networks. *IEEE Internet Things J.* **2021**, *8*, 9814–9826. [[CrossRef](#)]
27. Chen, W.; Wang, Y.; Yuan, Y. Combinatorial Multi-Armed Bandit: General Framework and Applications. In Proceedings of the 30th International Conference on Machine Learning, Atlanta, GA, USA, 17–19 June 2013; Dasgupta, S., McAllester, D., Eds.; Proceedings of Machine Learning: Pittsburgh, PA, USA; Volume 28, pp. 151–159.
28. Sinha, D.; Sankararama, K.A.; Kazerouni, A.; Avadhanula, V. Multi-Armed Bandits with Cost Subsidy. In Proceedings of the AISTATS, Virtual, 18 September 2021.
29. Li, F.; Liu, J.; Ji, B. Combinatorial Sleeping Bandits With Fairness Constraints. *IEEE Trans. Netw. Sci. Eng.* **2020**, *7*, 1799–1813. [[CrossRef](#)]
30. Mohamed, E.M.; Hashima, S.; Hatano, K.; Kasban, H.; Rihan, M. Millimeter-Wave Concurrent Beamforming: A Multi-Player Multi-Armed Bandit Approach. *Comput. Mater. Contin.* **2020**, *65*, 1987–2007. [[CrossRef](#)]
31. Mohamed, E.M.; Hashima, S.; Aldosary, A.; Hatano, K.; Abdelghany, M.A. Gateway Selection in Millimeter Wave UAV Wireless Networks Using Multi-Player Multi-Armed Bandit. *Sensors* **2020**, *20*, 3947. [[CrossRef](#)]
32. Beyer, H.G.; Schwefel, H.P.; Wegener, I. How to analyze evolutionary algorithms. *Theor. Comput. Sci.* **2002**, *287*, 101–130. [[CrossRef](#)]

Disclaimer/Publisher’s Note: The statements, opinions and data contained in all publications are solely those of the individual author(s) and contributor(s) and not of MDPI and/or the editor(s). MDPI and/or the editor(s) disclaim responsibility for any injury to people or property resulting from any ideas, methods, instructions or products referred to in the content.